Tribology Letters (2023) 71:1
https://doi.org/10.1007/s11249-022-01676-2

ORIGINAL PAPER

Preparation of Nanofluid of Lanthanum Borate Nanosheets and Investigation of Its Tribological Properties and Tribomechanisms in Different Base Oils

Jing Wu[1] · Guangbin Yang[1] · Shengmao Zhang[1] · Yujuan Zhang[1] · Lu Sun[1] · Tianhua Sun[1] · Laigui Yu[1] · Pingyu Zhang[1]

Received: 7 October 2022 / Accepted: 6 November 2022 / Published online: 23 November 2022

Abstract
Oleic acid-modified lanthanum borate nanosheets (OA-LBNs) were prepared by simple surface modification technology combined with precipitation method. The structure of the as-prepared light yellow transparent nanofluid of OA-LBNs was analyzed by Fourier transform infrared spectroscopy and transmission electron microscopy, and its thermal stability was evaluated by thermogravimetric analysis. Moreover, the tribological properties of OA-LBNs nanofluid as the lubricant additive in diisooctylsebacate (DIOS), poly-α-olefin (PAO4), and rapeseed oil (RO) were evaluated with a four-ball friction and wear tester, and its tribomechanisms in the three kinds of base oils were also discussed. The results show that OA-LBNs nanofluid exhibits good antiwear ability in the three kinds of base oils; in particularly, OA-LBNs nanofluid added in PAO4 shows the best antiwear ability. The tribological properties of the OA-LBNs nanofluid as the lubricant additive are dependent on the nature of the base oils. Namely, the polarity of the base oil influences the adsorption of the OA-LBNs nanofluid on the rubbed steel surface, thereby affecting the composition of the tribofilm formed on the rubbed steel surface and resulting in changes in tribological properties.

Keywords Lanthanum borate nanosheets · Nanofluid · Preparation · Tribological properties · Tribomechanism

1 Introduction

Lubricating oil is essential in most mechanical systems for reducing friction and wear, improving fuel efficiency of machinery, increasing service life of mechanical equipment, and reducing energy consumption [1–4]. Among conventional additives, sulfur, phosphorus, and chlorine are the most important elements used to improve the extreme pressure and antiwear properties of lubricating oil. However, these active elements in the lubricant additive are harmful to environment [5, 6]; and it is urgent to develop environmentally friendly additives with excellent extreme pressure properties and antiwear ability to replace S-, P-, and Cl-containing conventional additives. In this sense, nanoadditives could be of special significance, due to their excellent mechanical strength, high thermal stability, and good antiwear ability. For example, TiO_2-reinforced boron and nitrogen co-doped reduced graphene oxide is reported to be an efficient antiwear additive even at a low concentration, while graphene oxide film as a solid lubricant is said to have good lubricity [7, 8].

Similarly, borates have been widely studied and applied as lubricant additives, due to their good extreme pressure properties, friction-reducing and antiwear abilities, oxidation stability and anti-corrosion ability, as well as excellent load-carrying capacity and non-toxicity in association with a certain degree of biodegradability [9, 10]. This, in combination with the versatility and good compatibility of borates with other additives, could make it feasible to formulate green lubricant additives by replacing environment-harmful elements such as S, P, and Cl with B [11]. Zhao et al. [12] added surface modifiers hexadecyltrimethoxysilane and oleic acid in the preparation process of zinc borate ultrafine powder; and the as-obtained surface-capped zinc borate nanoparticles as the lubricant additive in liquid paraffin can drastically reduce the wear scar diameter and

✉ Guangbin Yang
yang0378@henu.edu.cn

✉ Pingyu Zhang
pingyu@henu.edu.cn

[1] Engineering Research Center for Nanomaterials, Henan University, Kaifeng 475004, Henan, China

friction coefficient. Jia et al. [13] synthesized a series of calcium borate/graphene oxide (CB/GO) composites via the hydrothermal treatment of borax, calcium nitrate and graphene oxide; and they found that the as-prepared composites can effectively improve the friction-reducing and antiwear abilities of poly-alpha olefin (PAO) base stock. Hao et al. prepared oleic acid-capped calcium borate by direct precipitation method to acquire increased oil-solubility; and they found that the as-prepared calcium borate as the additive of MVIS 250 base oil exhibits good antiwear and friction-reducing properties [14]. Lin et al. prepared nano lanthanum borates with different morphology (sheet-like, petal-like and ball-like) by hydrothermal method [15]; and they said that the tribological properties of the as-prepared nano lanthanum borates as lubricant additive are dependent on its morphology. Particularly, the sheet-like lanthanum borate has more chance than spherical one to react with worn steel surface and generate a tribochemical film, thereby exerting better triboeffects.

Usually, various boron compounds exhibit structure diversity, of them borate as the lubricant additive may function via forming deposition film and boronizing as well. Some researchers suggest that borate additives are transformed into boric acid in an acidic medium, and the as-formed boric acid participates in tribochemical reaction to form B_2O_3 on the rubbed surfaces, thereby reducing friction and wear. Gu et al. [16] said that lanthanum borate nanorods modified by oleic acid can significantly improve the friction-reducing and antiwear abilities of rapeseed oil, which is attributed to the formation of the adsorption film of oleic acid-modified lanthanum borate on the rubbed steel surfaces and of the complex boundary lubricating film dominated by Fe_2O_3, B_2O_3 and La_2O_3 upon tribochemical reaction thereon. Hu et al. [17] claimed that lanthanum borate is decomposed to form B_2O_3 under the shearing effect and extreme pressure effect while FeB is generated through further tribochemical reactions between B_2O_3 and iron friction pair; and the deposited film and tribochemical reaction film form a composite protective film on the friction surface to provide excellent load-carrying capacity. However, Qiao et al. [18] argued that there are no borates, boric acid or boron oxide on the rubbed steel surface; and instead, boron interstitial compound Fe_xB_y is present at the subsurface of the friction pair and can dissolve free boron to form a solid solution. The as-formed solid solution and iron oxides form a complex permeation layer on the rubbed steel surface to play a role in reducing friction and wear.

Nanofluid has a wide range of applications in tribology, because of its fluidity at room temperature and good dispersibility in oil [19–22]. In the present research, a solvent-free nanofluid made of oleic acid (OA)-capped lanthanum borate nanosheets (OA-LBNs) is prepared by a simple and facile liquid-phase method in the presence of oleic acid as the modifier. This paper reports the preparation of the OA-LBNs nanofluid and the investigation of its tribological properties and tribomechanisms in different base oils.

2 Experimental

2.1 Materials

Analytical reagents $Na_2B_4O_7{\cdot}10H_2O$ and $La(NO_3)_3{\cdot}6H_2O$ were supplied by Shanghai Aladdin Biochemical Technology Company Limited. Oleic acid was provided by Tianjin Kemiou Chemical Reagent Company Limited. Rapeseed oil (RO, food grade) was ordered from Shanghai Fulinmen Food Company Limited. Poly-alpha-olefin (PAO4) was obtained from Exxon Mobil Corporation, and diisooctylsebacate (DIOS) was supplied by Qingdao Zhongke Runmei Lubrication Material Technology Company Limited. All chemicals were used without further purification. The physicochemical parameters of the three base oils are shown in Table 1.

2.2 Preparation and Characterization of Nanofluid of OA-LBNs

OA-LBNs nanofluid was prepared by a liquid-phase method. Briefly, 5 mL of xylene and 1.3 mL (4 mmol) of oleic acid were added to a 100-mL three-necked flask. Then 20 mL of $La(NO_3)_3$ aqueous solution (0.1 mol/L) was poured into the flask; and the mixed solution was heated to 70 °C under magnetic stirring while 10 mL of $Na_2B_4O_7$ (0.22 mol/L) solution was added dropwise into the flask and the mixed reaction solution was held at 70 °C for 3 h to accompany its color change from milky white to transparent pale yellow. The upper layer of yellow transparent liquid was collected with a separating funnel, and then vacuum rotary-evaporated to obtain a yellow viscous liquid, the OA-LBNs nanofluid. The optical photograph of the OA-LBNs nanofluid is shown in Fig. 1. The target product is a viscous light yellow

Table 1 Physicochemical parameters of base oil

Parameters	Rapeseed oil	PAO4	DIOS
Density (15 °C, g/cm^3)	0.866	0.768	0.856
Dynamic viscosity (mm^2/s)			
40 °C	45.60	15.05	10.41
100 °C	10.07	3.20	2.76
Viscosity Index	180	128	154
Pour point (°C)	− 12	− 68	− 41
Flash point (°C)	252	246	210
Acid value (mgKOH/g)	≤ 1.0[a]	≤ 0.03	≤ 0.21

[a]The acid value of rapeseed oil is come from national standard of China "Rapeseed Oil" (GB/T 1536-2021)

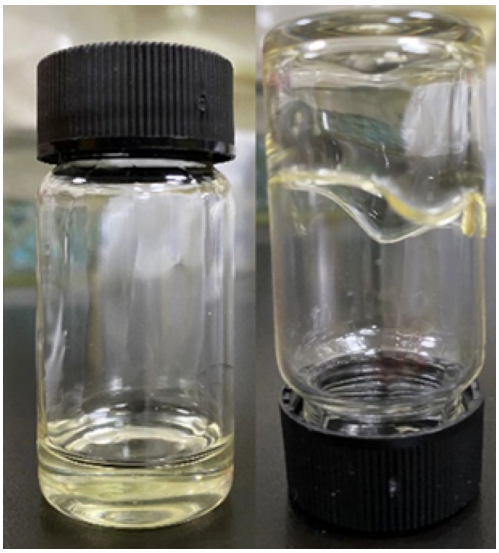

Fig. 1 Optical photo of OA-LBNs nanofluid

transparent nanofluid with a certain degree of flowability; and it is free of precipitation after centrifugation at 10,000 rev/min for 30 min, showing good stability. The unmodified nano lanthanum borate was prepared in the same method without the addition of oleic acid and xylene; and in this case the reaction solution remained white until the reaction was completed, and the white lanthanum borate nanoparticle (LBN) powder was obtained after centrifuging, washing and drying.

The morphology of the as-prepared samples was observed with a JEOL JEM-F200 transmission electron microscope (TEM, Japan); their crystal structure was analyzed by a D8 Advance X-ray powder diffractometer (XRD, Bruke, Germany) operating with $K\alpha$ radiation of Cu target at $\lambda = 1.54$ Å, acceleration voltage of 40 kV, current of 40 mA, step angle of 0.04°, step rate of 0.2 s, and scanning range of 5°–90°. A Vertex 70 Fourier transform infrared spectroscope (FTIR, Bruker, USA) was used to analyze the characteristic chemical groups of OA-LBNs in the wavenumber range of 400–4000 cm^{-1}. A TGA/SDTA851e thermogravimetric analyzer (TGA, Mettler Toledo, Switzerland) was used to analyze the thermal stability of the as-prepared samples from room temperature to 800 °C at a heating rate of 10 °C/min under nitrogen atmosphere. The element composition of the as-prepared OA-LBNs nanofluid was analyzed by X-ray photoelectron spectrometer (XPS, Kratoe, UK).

2.3 Friction and Wear Test

OA-LBNs nanofluid was separately dispersed in PAO4, DIOS, and RO base oils at different mass fractions, and the tribological properties of the resultant dispersions were evaluated with an MS-10RA four-ball friction and wear tester. The GCr15 bearing steel balls (Shanghai Steel Ball Company Limited) comprising the frictional pair have a diameter of 12.7 mm, a surface roughness of 0.05 μm, a Rockwell hardness of 59–64, an elastic modulus of 208 GPa, and a Poisson's ratio of 0.3. The sliding tests were run at a normal load of 392 N (corresponding to a Hertzian contact pressure of 2.30 GPa), a rotating speed of 1200 rev/min, and a temperature of 75 °C for a duration of 60 min (see ASTM D2266-2001).The wear scar diameter (WSD) of the three lower balls was measured using an optical microscope with a charge-coupled device (CCD) sensor connected to a computer; and the friction coefficient was automatically recorded by the computer. At the end of each sliding test, the frictional pair was disassembled, and the steel balls were cleaned 3 times with petroleum ether (boiling point 60–90 °C) in an ultrasonic bath.

The three-dimensional (3D) profiles and two-dimensional (2D) profiles of the wear scars were obtained with a contour GT-I white-light interfering profilometer (Bruker, Germany). The morphology of the wear scars on the steel balls was observed using a GeminiSEM 500 field emission scanning electron microscope (SEM) equipped with an energy dispersive spectrometer (EDS) accessory. The chemical composition and valence state of major elements on the worn surfaces of the steel balls were analyzed with an X-ray photoelectron spectroscope (XPS, Kratos, UK).

3 Results and Discussion

3.1 Characterization of OA-LBNs Nanofluid

Figure 2 presents the TEM images of unmodified lanthanum borate and OA-capped lanthanum borate. The unmodified lanthanum borate shows obvious sign of agglomeration (Fig. 2a), while the nanosheet-like OA-LBNs have a diameter of about 22 nm and a thickness of 6 nm and exhibit no obvious sign of agglomeration (Fig. 2b). It is generally recognized that oleic acid as the surface modifier can effectively prevent the growth of lanthanum borate nanoparticle in the reaction solution, and its long-chain alkyl group with excellent lipophilicity can improve the compatibility of the surface-capped inorganic nanoparticle with lubricant base oil.

XRD analysis of the as-prepared samples was carried out to identify their species and crystal type. As illustrated in Fig. 3, the diffraction peaks of OA-LBNs are very similar to those of the unmodified lanthanum borate, which demonstrates that the surface modifier OA has little effect on the crystal structure of lanthanum borate. Besides, the diffraction peaks of the unmodified lanthanum borate and OA-LBNs are weak, which is because their drying temperature (80 °C) is much lower than the crystallization

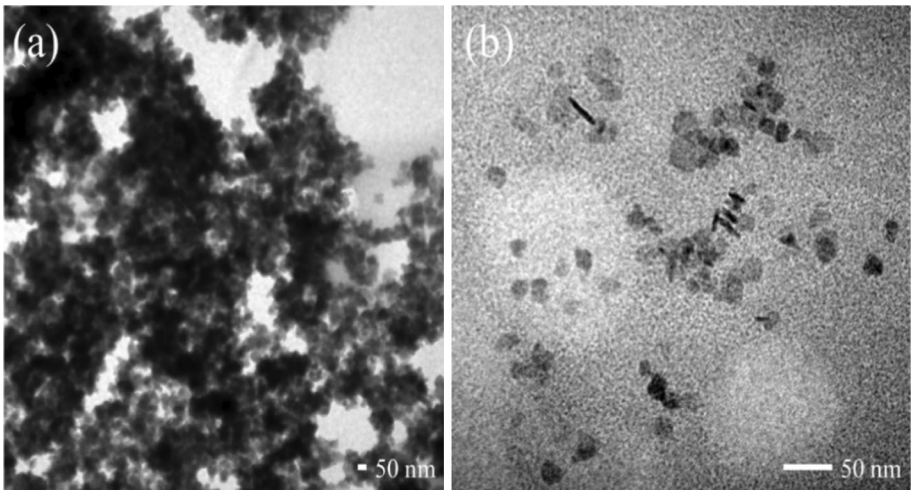

Fig. 2 TEM images of **a** unmodified lanthanum borate and **b** OA-capped lanthanum borate

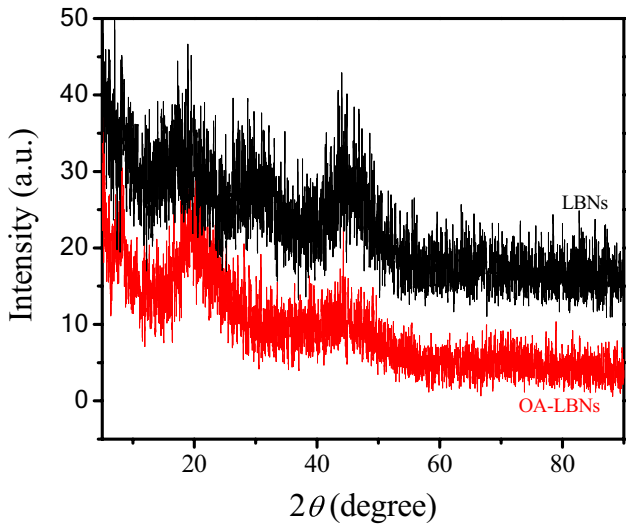

Fig. 3 XRD patterns of unmodified and OA-capped lanthanum borates

temperature of lanthanum borate (about 900 °C). Moreover, the diffraction peaks of OA-LBNs in the 2θ range of 5°–90° are broadened, which could be due to their small particle size associated with surface-modification by oleic acid or the formation of amorphous structure of lanthanum borate [23].

High-resolution XPS spectra were recorded to further analyze the element composition of the as-prepared OA-LBNs nanofluid. Figure 4 shows its B1s, C1s, O1s, and La3d XPS spectra. The strong double peaks at 838.0 eV and 853.0 eV are assigned to $La3d_{5/2}$ and $La3d_{3/2}$, respectively; the peak at 194 eV is attributed to B1s; and the peak at 528 eV is ascribed to O1s. Moreover, the C1s peak at 282.5 eV originates from oleic acid modifier and contaminant carbon. These XPS results further confirm the successful synthesis of the target product.

The interaction between the modifier and lanthanum borate was analyzed by FTIR spectrometry. As shown in Fig. 5, LBNs have absorbance peaks at 3438 cm^{-1} and 1649 cm^{-1}, due to the stretching vibration of hydroxyl groups in adsorbed water [24]. The hydroxyl peak of LBN modified by OA almost disappeared. The absorbance peaks of OA-LBNs nanofluid at 1307 cm^{-1} and 718 cm^{-1} and those of LBNs at 1384 cm^{-1} and 735 cm^{-1} correspond to the symmetrical stretching vibration of B-O and the bending vibration of B-O, respectively [25, 26]. In addition, the absorbance peaks of oleic acid and OA-LBNs nanofluid at 2925 cm^{-1} and 2856 cm^{-1} are attributed to the C–H stretching vibration of $–CH_3$ and $–CH_2–$, and the C–H bending vibration bands appear at 1420 cm^{-1} in FTIR spectrometry of oleic acid and 1416 cm^{-1} in that of OA-LBNs. However, the unmodified lanthanum borate does not show corresponding absorbance peaks. It is worth noting that the peak at 1709 cm^{-1} is caused by the carbonyl stretching vibration of OA, and this peak disappears in the FTIR spectrum of OA-LBNs nanofluid, which indicates that the oleic acid, –COOH has reacted with lanthanum borate completely. Furthermore, new absorbance band at 1544 cm^{-1} refers to the carbonyl (C=O) asymmetric stretching vibration (υ_{as}) of carboxylate ($–COO^-$) in OA-LBNs nanofluid, which proves that OA is modified onto the surface of LBNs via chemical bonding [16]. Furthermore, symmetric stretch vibration band (υ_s) of carboxylate ($–COO^-$) appears at 1457 cm^{-1}, and $\Delta\upsilon$ ($\upsilon_{as} - \upsilon_s$) value is smaller that the $\Delta\upsilon$ of bridging structure (120–160 cm^{-1}) [27]. These FTIR data demonstrate that oleic acid has been bonded to the O–H groups at the surface of lanthanum borate nanosheets with a monodentate carboxylates.

Figure 6 illustrates the TGA curves of OA-LBNs nanofluid and oleic acid. Oleic acid begins to lose weight at about 210 °C, and it completely loses weight at 360 °C. However, OA-LBNs nanofluid begins to lose weight at 310 °C, higher

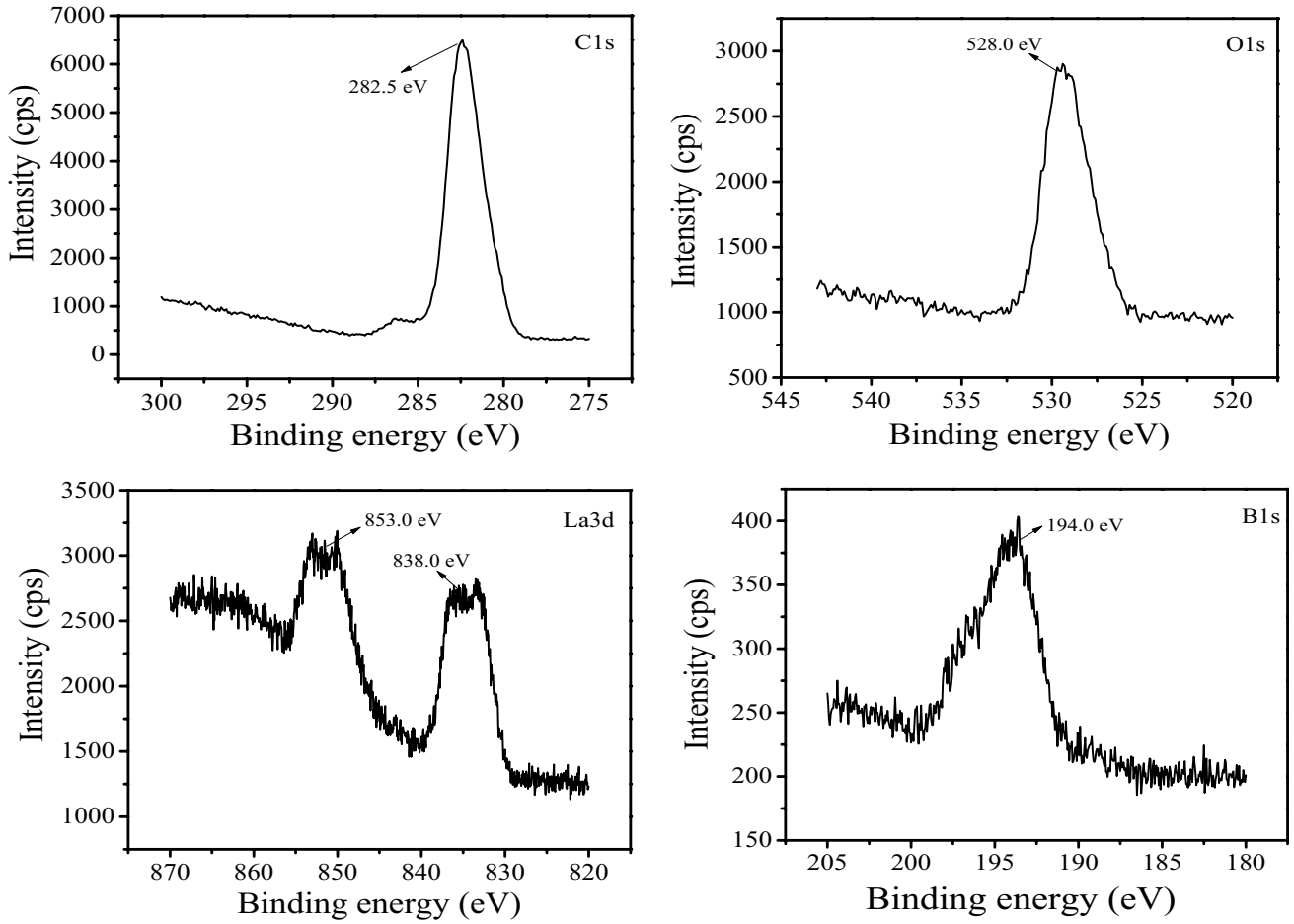

Fig. 4 B1s, C1s, O1s, and La3d XPS spectra of OA-LBNs nanofluid

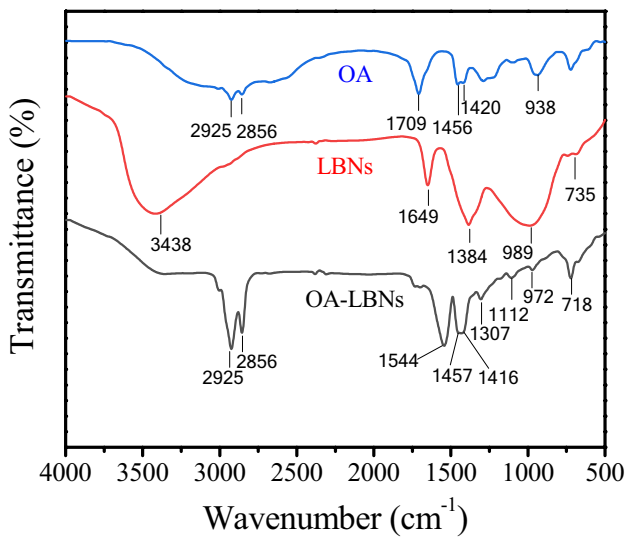

Fig. 5 FTIR spectra of OA, LBNs and OA-LBNs nanofluid

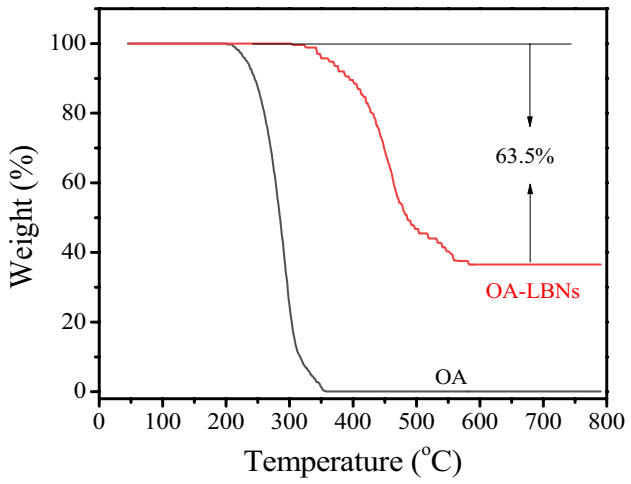

Fig. 6 TGA curves of oleic acid and OA-LBNs nanofluid

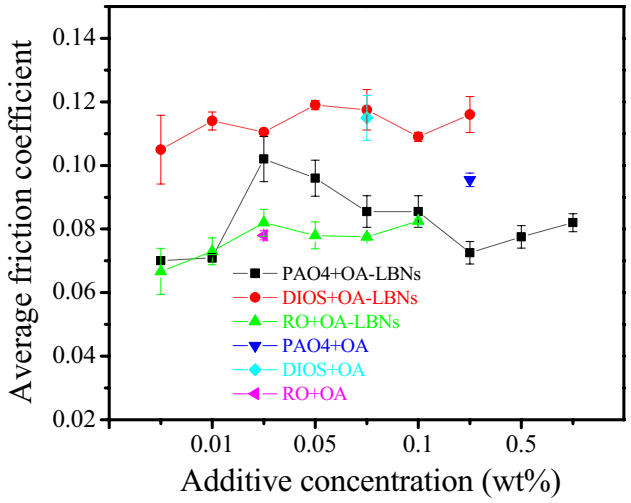

Fig. 7 Variation of friction coefficient with additive concentration in different base oils (four-ball friction and wear tester; load: 392 N; speed: 1200 rev/min; time: 60 min; temperature: 75 °C)

than that of oleic acid. This indicates that the grafting of oleic acid onto the surface of lanthanum borate by chemical bonding is favorable for improving the thermal stability of the inorganic nanosheet. Moreover, the complete weight loss of OA-LBNs nanofluid around 570 °C is about 63.5%, corresponding to its content of surface grafted OA.

3.2 Tribological Properties

Figure 7 depicts the relationship between the friction coefficient and additive concentration in PAO, DIOS and RO base oils, respectively. After the addition of OA-LBNs nanofluid in PAO4, the friction coefficient first increases and then decreases with the increase of the additive concentration, and it reaches the lowest value of 0.073 when the additive concentration is 0.3% (mass fraction), being equal to the friction coefficient under the lubrication of PAO4 alone (0.070). This indicates that OA-LBNs nanofluid has a negative effect on the friction-reducing behavior of the PAO4 base oil. On the one hand, the OA-LBNs nanofluid and the PAO4 base oil undergo competitive adsorption on the rubbed steel surfaces to form a boundary lubricating film thereon. On the other hand, OA-LBNs nanofluid may participate in tribochemical reactions with the freshly exposed steel surfaces during the sliding process, forming an adsorption film or tribofilm thereon. The shear strength or roughness of the as-formed composite film, however, is higher than that of the steel sliding pair, which results in an increase in the friction coefficient [28]. When OA-LBNs nanofluid is introduced into DIOS and RO, the friction coefficient curves are relatively stable with the increase of the additive concentration. This indicates that the friction-reducing effect of the OA-LBNs nanofluid as the additive in DIOS and RO is insignificant and nearly independent of its concentration. The reason might lie in that the DIOS and RO base oils have a stronger polarity than the OA-LBNs nanofluid, which is favorable for their preferential adsorption on the rubbed steel surfaces to inhibit the adsorption of the nanofluid thereon. However, among the three additive-free base oils, it is interesting that the friction coefficient under RO lubrication is the lowest (0.067), it is consistent with people's common understanding that vegetable oils possess better lubricity than PAO (0.070); while the friction coefficient under DIOS lubrication is the highest (0.105), which may be related to the nature of base oil and experimental conditions.

Figure 8 presents the relationship between the WSD and the concentration of OA-LBNs nanofluid in PAO4, DIOS, and RO base oils (four-ball friction and wear tester; load: 392 N; speed: 1200 rev/min; time: 60 min; temperature: 75 °C). Under the lubrication of PAO4 containing OA-LBNs nanofluid, the WSD decreases rapidly with the increase of the additive concentration and then levels off. When the additive concentration is 0.3%, the WSD reaches the lowest value of 0.36 mm, much smaller than that under the lubrication of PAO4 base oil (0.76 mm), and also smaller than the one under the lubrication of PAO4 containing 0.3% of oleic acid (0.66 mm). On the one hand, the introduction of an appropriate amount of OA-LBNs nanofluid leads to a significant improvement in the antiwear ability of PAO4, since the additive can easily enter the rubbed steel surfaces to form a deposited film thereon under local high flash temperature and high contact pressure. The as-formed surface protective film contributes to preventing the direct contact between the rubbed surfaces and greatly reducing wear [29]. On the other hand, the best antiwear ability occurs at a certain additive

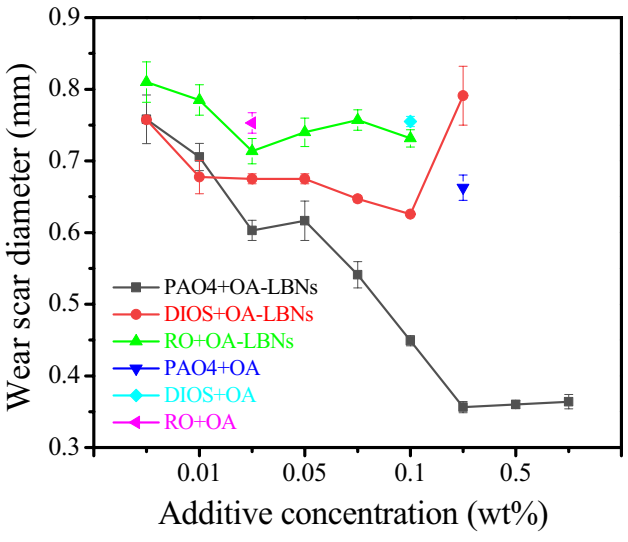

Fig. 8 Variation of wear scar diameter with additive concentration in different base oils (sliding condition the same as that of Fig. 7)

concentration at which the adsorbed film could be arranged more closely and densely on the rubbed steel surfaces. Beyond that concentration, however, the adsorption and desorption of the lubricant additive on the rubbed steel surfaces reach a dynamic balance, and hence the WSD levels off with further increasing additive concentration [30].

When OA-LBNs nanofluid is used as the additive of DIOS base oil, the WSD reaches a minimum of 0.63 mm at an additive concentration of 0.1%, lower than that under the lubrication of DIOS base oil (0.76 mm), and also lower than the one under the lubrication of DIOS containing 0.1% of oleic acid (0.76 mm). As the additive concentration further increases, the antiwear performance deteriorates, possibly due to the agglomeration of the too high concentration of OA-LBNs with a high surface energy and a high intermolecular force. The aggregates of OA-LBNs nanofluid in the DIOS base oil could cause three-body abrasive wear, thereby resulting in increase in wear [31]. However, the antiwear performance does not change significantly when OA-LBNs nanofluid is introduced into RO base oil. For example, the WSDs under the lubrication of RO with 0.03% of OA-LBNs nanofluid and with 0.03% of oleic acid (0.71 mm and 0.75 mm) are close to that under the lubrication of RO base oil (0.81 mm). In general, OA-LBNs nanofluid in DIOS and RO base oils is less effective than in PAO4 base oil in terms of its antiwear ability for the steel-steel sliding pair. This could be related to its competitive adsorption with DIOS and RO base oils on the rubbed steel surfaces. Namely, both DIOS and RO with a high polarity can be chemically adsorbed on the rubbed steel surfaces to generate a relatively thick oil film with a low shear stress. When the additive concentration is low, DIOS and RO are preferentially adsorbed on the rubbed metal surfaces as the main adsorbates, resulting in a stable tribofilm thereon to reduce the friction and wear of the steel-steel sliding pair. While the additive concentration is too high, OA-LBNs nanofluid tends to agglomerate, thereby damaging the compactness and continuity of the oil film as well as antiwear ability [32]. Previous researches demonstrate that lubricant additives such as oil-soluble nano-Cu with a relatively low melting point [33, 34] and functionalized BN nanosheets [35, 36] have good friction-reducing and antiwear properties. This is because the surface modifier of the oil-soluble nano-Cu plays a role in reducing the friction coefficient while the Cu nanocore plays a role in load-carrying during the friction process [33, 34]. Similarly, molybdenum dialkyldithiocarbamate (MoDTC), a common lubricant additive, exhibits excellent friction-reducing ability in PAO base oil, because it forms a surface layer of MoS_2 nanocrystal with a low shear strength; its antiwear ability in the same base oil, however, is relatively poor [37, 38]. Different from MoDTC, traditional engine oil additive zinc dialkyldithiophosphate (ZDDP) [39], borate ester [40], ZnO nanoparticle [41], and CeO_2 nanoparticle [42] have significant antiwear ability but poor friction-reducing ability, since they often form tribofilms with a high shear strength.

The plot of wear scar diameter as a function of applied load is shown in Fig. 9. Under the same load, the WSD under the lubrication of pure PAO4 is relatively large. Under the lubrication of PAO4 containing 0.3% OA-LBNs nanofluid, the WSD decreases to a certain extent within the tested load range. This indicates that OA-LBNs nanofluid can improve the antiwear ability of PAO4 under the applied load from 196 to 490 N. On the whole, the variation trend of WSD versus load under the lubrication of pure PAO4 and PAO4 containing 0.3% OA-LBNs nanofluid is similar: the WSD initially decreases and then increases with increasing load. When the load is lower than 294 N, the WSD decreases with the increase of the load, because the elastohydrodynamic fluid effect of the base oil is significant at low loads while the additive can form chemically adsorbed film to reduce wear thereat. When the load is above 294 N, the WSD tends to increase with further increase of the load, which is due to the decrease in the thickness of the tribofilm in association with the increase in the direct contact area of the friction pair thereat [43].

Figures 10 and 11 exhibit the 3D and 2D profiles of the worn surfaces of lower steel balls lubricated by different base oils without or with OA-LBNs nanofluid. The WSD of the lower steel balls lubricated by pure base oils is large, and there are many wide and deep furrows along the sliding direction (Fig. 10a1, b1 and c1); under the lubrication of the base oils containing OA-LBNs nanofluid, the WSD is relatively small. In particular, under the lubrication of PAO4 base oil containing 0.3% of OA-LBNs nanofluid, the WSD is the smallest. This is mainly because

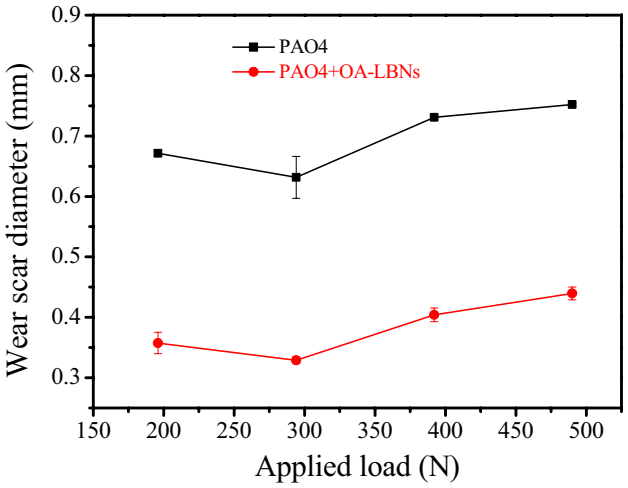

Fig. 9 Variation of wear scar diameter with applied load under the lubrication of PAO4 and PAO4 containing 0.3% OA-LBNs nanofluid (sliding condition the same as that of Fig. 7)

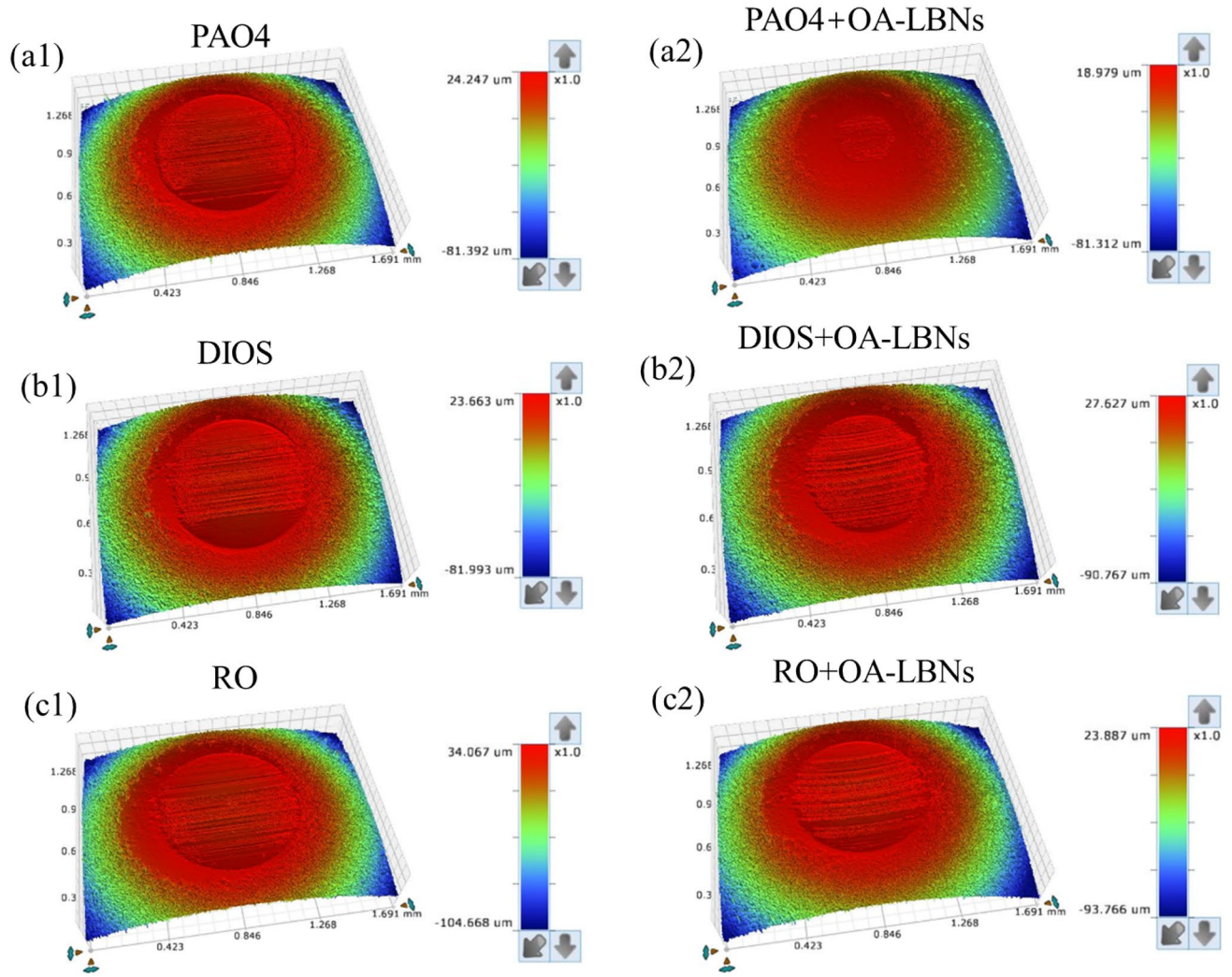

Fig. 10 3D topography of worn steel surfaces (sliding condition the same as that of Fig. 7)

OA-LBNs nanofluid as the additive in PAO4 base oil can be chemically adsorbed onto the friction surface to form a protective tribofilm, thereby avoiding the direct contact between sliding steel surfaces and reducing wear. Similar phenomenon is also visible in the 2D profiles of the worn surfaces: the depth of the wear scar under the lubrication of pure PAO4 is larger than that under the lubrication of PAO4 containing 0.3% OA-LBNs nanofluid.

To clarify the action mechanism of OA-LBNs additive in different base oils, we analyzed the morphology of the worn surfaces of the steel balls and the element composition of the tribofilm thereon by SEM–EDS. Figure 12 shows the SEM images and EDS element distributions of the worn surfaces of the steel balls lubricated by different base oils without or with OA-LBNs nanofluid. Similar to what is seen in Fig. 10, the WSDs of the steel balls lubricated by PAO4 (Fig. 12a1), DIOS (Fig. 12b1), and RO (Fig. 12c1) base oils are large; and deep furrows and plastic deformation are visible on the worn steel surfaces. This indicates that the sliding pair is dominated by abrasive wear and galling under the lubrication of the base oil alone. In other words, the lubricating film formed by the base oil alone has poor antiwear ability, possibly due to its poor strength. Compared to the worn steel surfaces lubricated by the base oil alone, those lubricated by the base oil with OA-LBNs nanofluid are relatively smooth and do not show signs of severe galling along the sliding direction (Fig. 12a2, b2, c2). This indicates that the as-synthesized OA-LBNs nanofluid as the additive in PAO4, DIOS, and RO base oils can reduce the wear of the steel balls to a certain extent.

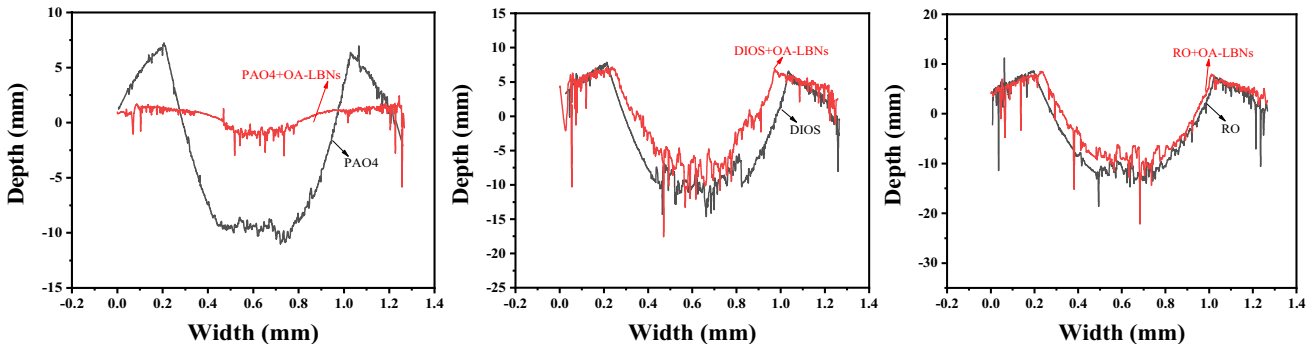

Fig. 11 2D depth profiles of worn steel surfaces (sliding condition the same as that of Fig. 7)

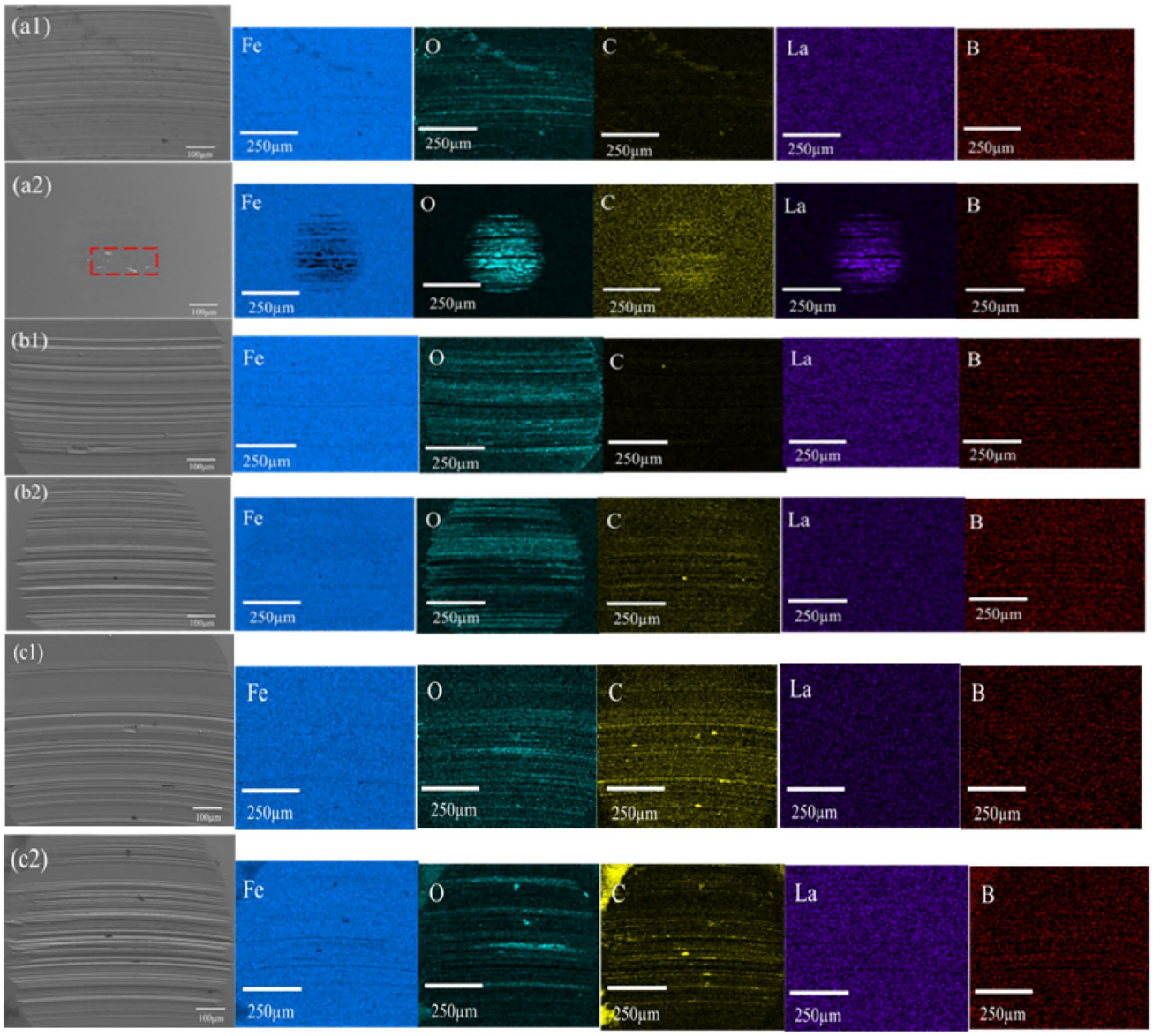

Fig. 12 SEM micrographs (left) and corresponding EDS element surface distribution mappings (right) of worn steel surfaces lubricated by (a1) PAO4, (a2) PAO4 + OA-LBNs, (b1) DIOS, (b2) DIOS + OA-LBNs, (c1) RO, and (c2) RO + OA-LBNs (sliding condition the same as that of Fig. 7)

It is worth mentioning that the wear scar of the steel ball under the lubrication of PAO4 with 0.3% OA-LBNs nanofluid is dominated by slight wear in association with narrow furrows and shallow scratches (Fig. 12a2), and it is smaller than those under the lubrication of DIOS or RO with OA-LBNs nanofluid (Fig. 10b2 and c2). As seen in Fig. 12a2 and Table 2, there is an obvious tribofilm as well as a large amount of O, La, and B elements on the worn surface of the steel ball lubricated by PAO4 containing 0.3% OA-LBNs nanofluid. Nevertheless, no obvious EDS signals of La and B elements are visible on the worn steel surfaces lubricated by DIOS or RO with OA-LBNs. This further proves that OA-LBNs nanofluid in DIOS and RO base oils are not easily enriched on the rubbed steel surface, corresponding to the friction and wear test data provided in Figs. 8 and 10.

The chemical composition of the tribofilm on the worn surface was further analyzed by XPS to reveal the tribomechanism of OA-LBNs nanofluid as the additive in different base oils. Figure 13 depicts the XPS spectra of typical elements on the worn steel surface under the lubrication of PAO4 containing 0.3% OA-LBNs nanofluid. The B1s peak at 192.3 eV is assigned to B_2O_3 [44], which indicates that B participates in tribochemical reaction during the friction process. It should be pointed out that the atomic number of element B is small, which corresponds to the less intense B1s spectrum. The C1s peaks at 284.8 eV and 285.5 eV correspond to C = C and C-O derived from the oleic acid modifier [45]. The XPS spectrum of O1s is fitted into three peaks located at 529.5 eV, 531.2 eV, and 533 eV, corresponding to the Fe–O bond, C=O/C–O bond, and B–O bond [46]. The Fe2p peaks at 710.2 eV, 711.4 eV, 714.4 eV and 724 eV are attributed to Fe_3O_4, FeOOH, Fe_xB_y and Fe_2O_3, respectively [47, 48], which demonstrates that the steel sliding pair also participates in tribochemical reactions. The La3d peaks at 835 eV and 838.6 eV are attributed to La_2O_3. These XPS results reveal that OA-LBNs nanofluid in PAO4 is initially adsorbed on the rubbed steel surface, then it takes part in complicated tribochemical reactions to generate a protective tribofilm containing Fe_2O_3, B_2O_3, La_2O_3, etc., thereby improving the antiwear performance of the PAO4 base oil.

Table 2 Element composition of worn steel surface

Lubricant	Element composition (%)					
	Fe	C	O	B	La	Other
PAO4 + OA-LBNs	51.31	5.88	15.84	7.35	18.44	1.17
DIOS + OA-LBNs	91.44	4.45	1.47	0.78	0.06	1.81
RO + OA-LBNs	84.14	9.59	3.36	1.10	0.00	1.82

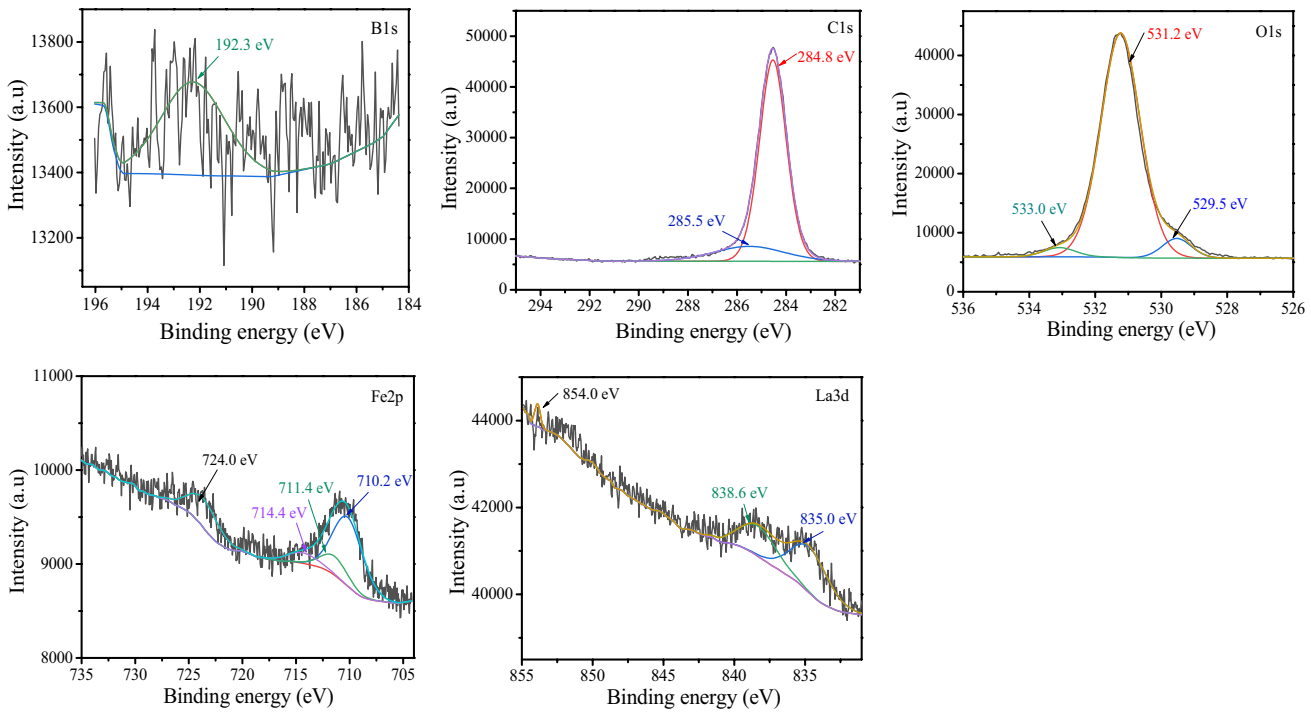

Fig. 13 XPS spectra of major elements on worn steel surface lubricated by PAO4 containing 0.3% OA-LBNs nanofluid

As to the worn steel surfaces lubricated by DIOS with OA-LBNs nanofluid or by RO with OA-LBNs nanofluid, the B1s and La3d XPS signals are very weak, which indicates that the OA-LBNs nanofluid in DIOS and RO base oils is poorly adsorbed onto the rubbed steel surface or prevented from participating in the tribochemical reactions. Relevant strong XPS signals of C1s, O1s and Fe2p (Fig. 14) suggest that the as-formed tribofilms consist of only iron oxides and C species derived from DIOS or RO base oil, as evidenced by corresponding EDS data in Table 2. The XPS spectra of the rubbed steel surface lubricated by DIOS with OA-LBNs nanofluid are similar to those of the rubbed steel surface lubricated by RO with OA-LBNs nanofluid.

Based on the above mentioned, it is evident that OA-LBNs nanofluid as additive in different base oils functions via different tribomechanisms; and its tribomechanism is closely dependent on the nature of the base oil. PAO4 base oil is weakly polar alkane synthetic oil, while DIOS and RO are esters and have stronger polarity than alkane. In particular, RO contains double bonds and carboxylic acids, which further enhance the polarity of the oil. The tribomechanisms of OA-LBNs nanofluid in different base oils are schematically illustrated in Fig. 15. There is a competitive adsorption between the additive and the base oil molecules on the steel sliding surface. OA-LBNs nanofluid has a stronger polarity than PAO4 base oil, and hence OA-LBNs nanofluid rather than PAO4 base oil is preferentially adsorbed onto the surface of the steel sliding pair. In the meantime, OA-LBNs nanofluid participates in tribochemical reactions in the presence of friction-induced heat and applied normal load to form a tribofilm composed of Fe_2O_3, B_2O_3, La_2O_3, etc., thereby improving the antiwear properties of the PAO4 base oil. Contrary to the above, DIOS and RO with polarity higher than that of OA-LBNs nanofluid become the dominant adsorbates on the rubbed steel surface during the competitive adsorption, while a small amount of OA-LBNs nanofluid adsorbed on the rubbed steel surface might disrupt the continuity of the oil film and damage the antiwear performance.

4 Conclusions

Light yellow transparent OA-LBNs nanofluid is prepared by a simple surface modification route in combination with precipitation method. The sheet-like nanocore of the as-prepared OA-LBNs nanofluid has a diameter of about 22 nm and a thickness of 6 nm. OA-LBNs nanofluid as the additive in PAO4, DIOS, and RO base oils can improve the antiwear behavior to varying extents; and its antiwear action is dependent on the polarity of the base oils, due to competitive adsorption on the rubbed steel surface. Particularly, it can significantly improve the antiwear performance of PAO4 base oil, because low polarity PAO4 does not seriously disturb the adsorption of OA-LBNs nanofluid as well as its participation in tribochemical reactions. The highly

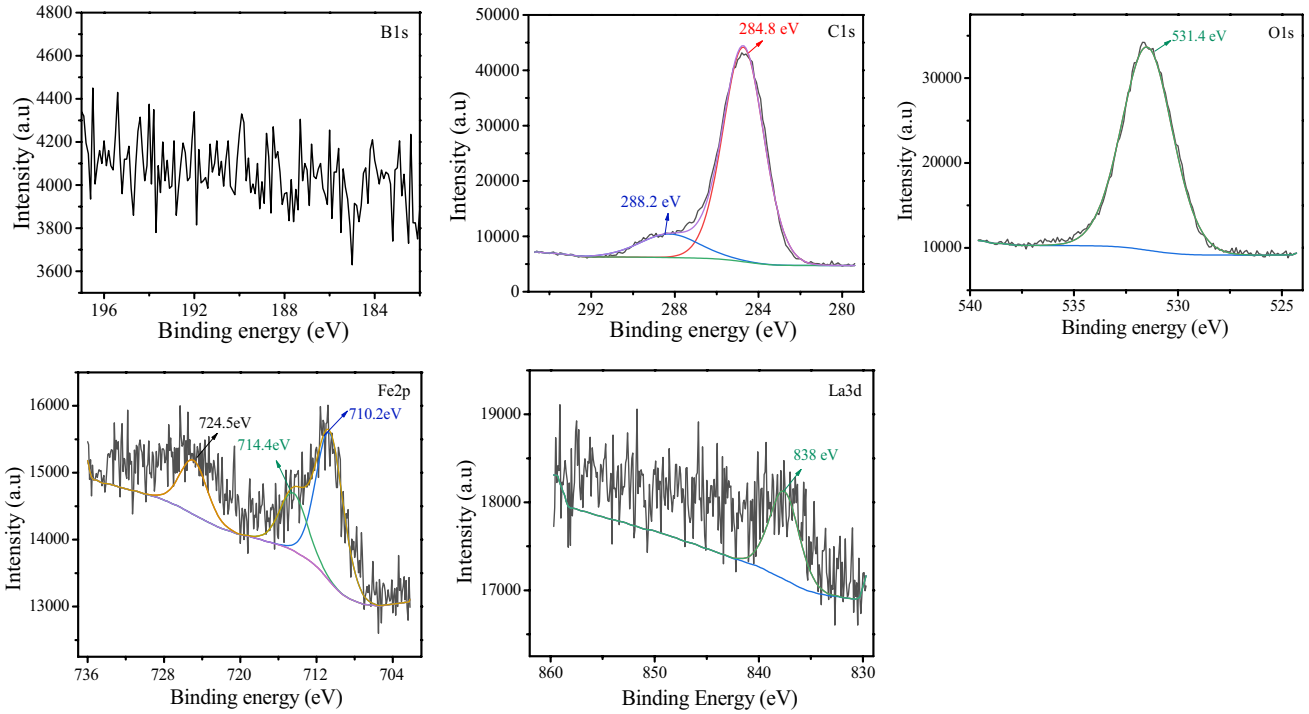

Fig. 14 XPS spectra of major elements on worn steel surface lubricated by RO with 0.03% OA-LBNs nanofluid

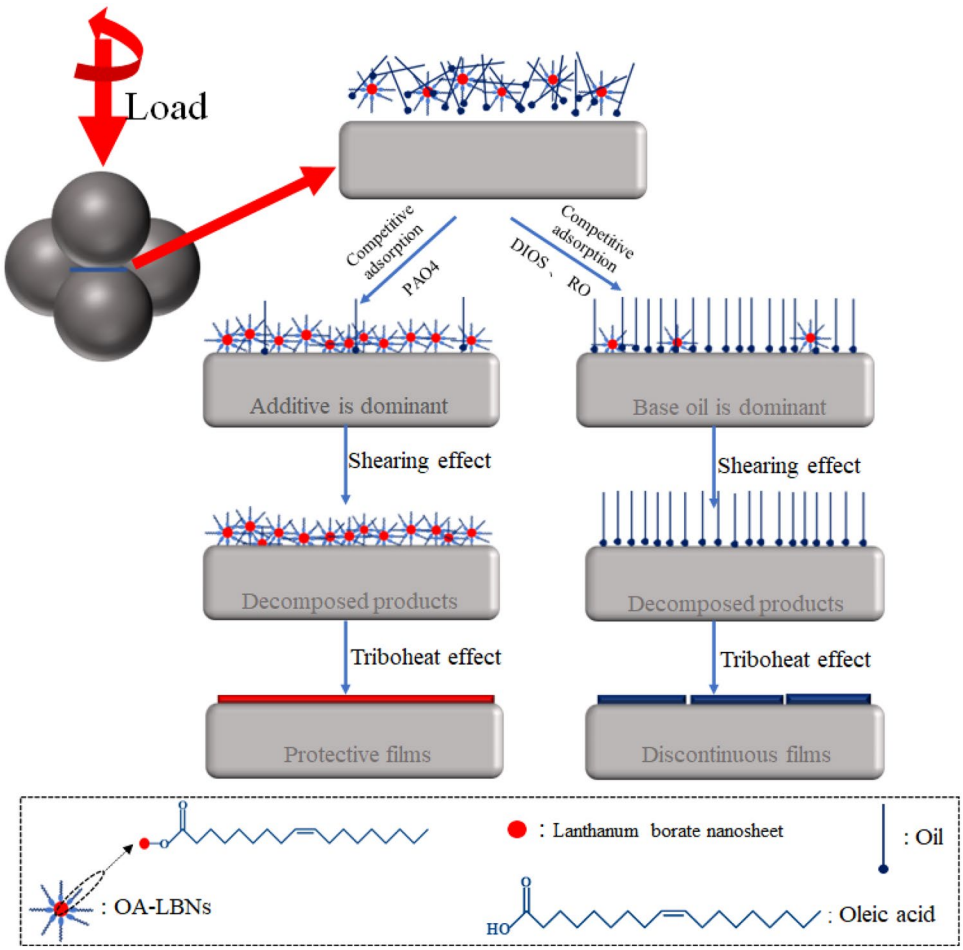

Fig. 15 Schematic diagram showing the tribomechanisms of OA-LBNs nanofluid in different base oils

polar molecules of DIOS or RO base oil, however, are preferentially adsorbed on the rubbed steel surface while the inclusion of a small amount of OA-LBNs nanofluid thereon might damage the integrity of the boundary lubrication film of the strongly polar base oil. This, in association with the inhibition of the tribochemical reactions involving the metal sliding pair, the base oil, and the lubricant additive, accounts for relatively insignificant antiwear ability of OA-LBNs nanofluid in DIOS or RO base oil.

Acknowledgements The authors acknowledge the financial support provided by National Natural Science Foundation of China (Grant No. 51875172), Zhongyuan Science and Technology Innovation Leadership Program (Grant No. 214200510024), the Tribology Science Fund of State Key Laboratory of Tribology (SKLTKF21B06), and Key Research and Development and Promotion Projects in Henan Province (No. 212102310410).

Author Contributions JW, preparation of Lanthanum Borate Nanofluids;GY, wrote the main manuscript text;SZ, prepared Figs. 4, 13 and 14, analyze friction mechanism;YZ, prepared Figs. 7, 8 and 9, evaluation of tribological properties;LS, prepared Figs. 10, 11 and 12, analysis of wear scar;TS, prepared Figs. 1, 2, 3, 4, 5 and 6, characterization of lanthanum borate nanofluids;LY, modify and touch up the main text;PZ, prepared Fig. 15, design the tribomechanisms of OA-LBNs nanofluid in different base oils.All authors reviewed the manuscript

Funding Funding were provided by the Tribology Science Fund of State Key Laboratory of Tribology (Grant Nos. SKLTKF21B06, SKLTKF21B06), Zhongyuan Science and Technology Innovation Leadership Program (Grant Nos. 214200510024, 214200510024), National Natural Science Foundation of China (Grant Nos. 51875172, 51875172) and Key Research and Development and Promotion Projects in Henan Province (Grant No. 212102310410).

Declarations

Competing interest The authors declare no competing interests.

References

1. Tung, S.C., McMillan, M.L.: Automotive tribology overview of current advances and challenges for the future. Tribol. Int. **37**(7), 517–536 (2004)
2. Chu, S., Majumdar, A.: Opportunities and challenges for a sustainable energy future. Nature **488**(7411), 294–303 (2012)
3. Holmberg, K., Andersson, P., Erdemir, A.: Global energy consumption due to friction in passenger cars. Tribol. Int. **47**, 221–234 (2012)
4. Wong, V.W., Tung, S.C.: Overview of automotive engine friction and reduction trends—effects of surface, material, and lubricant-additive technologies. Friction **4**(1), 1–28 (2016)

5. Rastogi, R.B., Maurya, J.L., Jaiswal, V.: Zero SAPs and ash free antiwear additives: schiff bases of salicylaldehyde with 1,2-phenylenediamine, 1,4-phenylenediamine, and 4,4′-diaminodiphenylenemethane and their synergistic interactions with borate ester. Tribol. Trans. **56**(4), 592–606 (2013)
6. Bhaumik, S., Maggirwar, R., Datta, S., Pathak, S.D.: Analyses of anti-wear and extreme pressure properties of castor oil with zinc oxide nano friction modifiers. Appl. Surf. Sci. **449**, 277–286 (2018)
7. Jaiswal, V., Kalyani, Umrao, S., Rastogi, R.B., Kumar, R., Srivastava, A.: Synthesis, characterization and tribological evaluation of TiO_2-reinforced boron and nitrogen co-doped reduced graphene oxide based hybrid nanomaterials as efficient antiwear lubricant additives. ACS Appl. Mater. Int. **8**(18), 11698–11710 (2016)
8. Liang, H.Y., Bu, Y.F., Zhang, J.Y., Cao, Z.Y., Liang, A.: Graphene oxide film as solid lubricant. ACS Appl Mater. Int. **5**(13), 6369–6375 (2013)
9. Wang, H.M., Zhang, Z.J.: Current status and progress of research on borate lubricant additives. Chem. Res. **22**(1), 104–107 (2011). ((**in Chinese**))
10. Li, J.S., Xu, J.: Research situation and development trends of nanosized borates used as lubricating additives. Lubr. Oil **30**(1), 37–41 (2015). ((**in Chinese**))
11. Ma, G.G., Ma, X.F., Zhang, C.C., Liu, J., Liu, X.W.: Expanding the borate additives to accelerate the transformation and upgrading of lubricating oil and agent. Lubr. Oil **30**(3), 12–20 (2015). ((**in Chinese**))
12. Zhao, C., Chen, Y.K., Jiao, Y., Loya, A., Ren, G.G.: The preparation and tribological properties of surface modified zinc borate ultrafine powder as a lubricant additive in liquid paraffin. Tribol. Int. **70**, 155–164 (2014)
13. Jia, Z.F., Pang, X.J., Li, H.Y., Ni, J.J., Shao, X.: Synthesis and wear behavior of oleic acid capped calcium borate/graphene oxide composites. Tribol. Int. **90**, 240–247 (2015)
14. Hao, L.F., Li, J.S., Xu, X.H., Ren, T.H.: Preparation and tribological properties of a kind of lubricant containing calcium borate nanoparticles as additives. Ind. Lubr. Tribol. **64**(1), 16–22 (2012)
15. Lin, W., Gu, K.C., Chen, B.S., Wang, X.: The tribological properties of lanthanum borate nanoparticles with different morphologies as lubricant additive in rapeseed oil. In: IOP Conference Series: Materials Science and Engineering **612**, 022019 (2019)
16. Gu, K.C., Chen, B.S., Wang, X.M., Wang, J., Fang, J.H., Wu, J., Huang, L.C.: Preparation, friction and wear properties of hydrophobic lanthanum borate nanorods in rapeseed oil. Trans. Nonferrous Met. Soc. China **24**(11), 3578–3584 (2014)
17. Hu, Z.S., Dong, J.X., Chen, G.X., He, J.Z.: Preparation and tribological properties of nanoparticle lanthanum borate. Wear **243**, 43–47 (2000)
18. Qiao, Y.L., Xu, B.S., Ma, S.L., Liu, W.M., Xue, Q.J.: Study on tribochemical mechanisms of the modified borate additives. Tribology **21**(6), 416–420 (2001). ((**in Chinese**))
19. Bourlinos, A.B., Ray Chowdhury, S., Herrera, R., Jiang, D.D., Zhang, Q., Archer, L.A., Giannelis, E.P.: Functionalized nanostructures with liquid-like behavior: expanding the gallery of available nanostructures. Adv. Funct. Mater. **15**(8), 1285–1290 (2005)
20. Gu, S.Y., Zhang, Y.H., Yan, B.B.: Solvent-free ionic molybdenum disulfide (MoS_2) nanofluids with self-healing lubricating behaviors. Mater. Lett. **97**, 169–172 (2013)
21. Guo, Y.X., Guo, L.H., Li, G.T., Zhang, L.G., Zhao, F.Y., Wang, C., Zhang, G.: Solvent-free ionic nanofluids based on graphene oxide-silica hybrid as high-performance lubricating additive. Appl. Surf. Sci. **471**, 482–493 (2019)
22. Liu, J.X., Wang, X., Liu, Y., Liu, X.Y., Fan, K.: Bioinspired three-dimensional and multiple adsorption effects toward high lubricity of solvent-free graphene-based nanofluid. Carbon **188**, 166–176 (2022)
23. Lin, W., Chen, B.S., Fang, J.H., Gu, K.C., Wu, J.: Influence of sizes on tribological properties and tribofilm formation of lanthanum borate nanospheres in soybean oil. Mater. Sci. Eng. **235**(10), 2184–2199 (2021)
24. Koksal, E., Afsin, B., Tabak, A., Caglar, B.: Structural characterization of aniline-bentonite composite by FTIR, DTA/TG, and PXRD analyses and BET measurement. Spectrosc. Lett. **44**(2), 77–82 (2011)
25. Peak, D., Luther, G.W., Sparks, D.L.: ATR-FTIR spectroscopic studies of boric acid adsorption on hydrous ferric oxide. Geochim. Cosmochim. Ac. **67**(14), 2551–2560 (2003)
26. Sun, N.J., Wang, C., Jiao, L.Y., Zhang, J., Zhang, D.H.: Controllable coating of boron nitride on ceramic fibers by CVD at low temperature. Ceram. Int. **43**(1), 1509–1516 (2017)
27. Deacon, G.B., Philips, R.J.: Relationships between the carbon-oxygen stretching frequencies of carboxylate complexes and the type of carboxylate coordination. Coord. Chem. Rev. **33**, 227–250 (1980)
28. Jin, F.J., Yang, G.B., Song, S.Y., Zhang, S.M., Yu, L.G., Zhang, P.Y.: Synthesis of nanostructured lanthanum fluoborate modified by oleylamine and evaluation of its tribological properties as a lubricating additive in synthetic ester. Surf. Interface Anal. **48**(10), 1033–1039 (2016)
29. Jiang, Z.Q., Zhang, Y.J., Yang, G.B., Ma, J.Y., Zhang, S.M., Yu, L.G., Zhang, P.Y.: Tribological properties of tungsten disulfide nanoparticles surface-capped by oleylamine and maleic anhydride dodecyl ester as additive in diisooctylsebacate. Ind. Eng. Chem. Res. **56**(6), 1365–1375 (2017)
30. Wang, S., Yue, W., Fu, Z.Q., Wang, C.B., Li, X.L., Liu, J.J.: Study on the tribological properties of plasma nitrided bearing steel under lubrication with borate ester additive. Tribol. Int. **66**, 259–264 (2013)
31. Chen, X.R., Chen, W.T., Zhang, L.Y., Zeng, M.L., Yang, S.M., Yang, Z.H., Ola, O., Thummavichai, K., Wang, N., Zhu, Y.: Implanting MnO_2 into hexagonal boron nitride as nanoadditives for enhancing tribological performance. Crystals **12**(4), 451 (2022)
32. Yang, G.B., Zhao, J.H., Cui, L., Song, S.Y., Zhang, S.M., Yu, L.G., Zhang, P.Y.: Tribological characteristic and mechanism analysis of borate ester as a lubricant additive in different base oils. RSC Adv. **7**(13), 7944–7953 (2017)
33. Guo, Z.Q., Zhang, Y.J., Wang, J.C., Gao, C.P., Zhang, S.M., Zhang, P.Y., Zhang, Z.J.: Interactions of Cu nanoparticles with conventional lubricant additives on tribological performance and some physicochemical properties of an ester base oil. Tribol. Int. **141**, 105941 (2020)
34. Zhang, Y.S., Xu, S.R., Zhao, Z.S., Shi, J., Zhao, Y., Zhang, G.G., Wu, Z.G.: Mass-produced Cu nanoparticles as lubricant additives for reducing friction and wear. Lubr. Sci. **34**(4), 235–246 (2022)
35. Wang, L.X., Han, W.F., Ge, C.C., Zhang, R., Bai, Y.F., Zhang, X.D.: Covalent functionalized boron nitride nanosheets as efficient lubricant oil additives. Adv. Mater. Interfaces **6**(21), 1901172 (2019)
36. Wu, H.X., Yin, S.C., Du, Y., Wang, L.P., Yang, Y., Wang, H.F.: Alkyl-functionalized boron nitride nanosheets as lubricant additives. ACS Appl. Nano Mater. **3**(9), 9108–9116 (2020)
37. Zhang, S.J., Zhu, L.N., Wang, Y.Y., Kang, J.J., Wang, H.D., Ma, G.Z., Huang, H.P., Zhang, G.A., Yue, W.: Effects of annealing treatment on tribological behavior of tungsten-doped diamond-like carbon film under lubrication (Part 2): tribological behavior under MoDTC lubrication. Friction **10**(7), 1061–1077 (2022)
38. Spikes, H.: Friction modifier additives. Tribol. Lett. **60**(1), 5 (2015)

39. Lei, X., Zhang, Y.J., Zhang, S.M., Yang, G.B., Zhang, C.L., Zhang, P.Y.: Study on the mechanism of rapid formation of ultra-thick tribofilm by CeO_2 nano additive and ZDDP. Friction (2022). https://doi.org/10.1007/s40544-021-0571-8
40. Yang, G.B., Zhang, Z.M., Li, G.H., Zhang, J.F., Yu, L.G., Zhang, P.Y.: Synthesis and tribological properties of S- and P-free borate esters with different chain lengths. J. Tribol. **133**(2), 021801 (2011)
41. Zhang, Y.Y., Zhang, Y.J., Zhang, S.M., Yang, G.B., Gao, C.P., Zhou, C.H., Zhang, P.Y.: One step synthesis of ZnO nanoparticles from ZDDP and its tribological properties in steel-aluminum contacts. Tribol. Int. **141**, 105890 (2020)
42. Wu, L.L., Lei, X., Zhang, Y.J., Zhang, S.M., Yang, G.B., Zhang, P.Y.: The tribological mechanism of cerium oxide nanoparticles as lubricant additive of poly-alpha olefin. Tribol. Lett. **68**(4), 68–101 (2020)
43. Li, J.S., Zhang, L.: Application studies of surface modified TiO_2 nanoparticles as additive in gear oil. Lubr. Oil **28**, 22–24 (2013). (**(in Chinese)**)
44. Jia, Z.F., Xia, Y.Q., Shao, X., Du, S.M.: Synthesis, characterization and tribological behavior of oleic acid-capped core-shell lanthanum borate-SiO_2 composites. Ind. Lubr. Tribol. **66**(1), 1–8 (2014)
45. Han, S., Liu, S.Z., Wang, Y.H., Zhou, X.L., Hao, L.F.: Preparation, characterization, and tribological evaluation of a calcium borate embedded in an oleic acid matrix. Ind. Eng. Chem. Res. **51**(43), 13869–13874 (2012)
46. Ji, X.B., Chen, Y.X., Wang, X.B., Liu, W.M.: Tribological behaviors of novel tri(hydroxymethyl)propane esters containing boron and nitrogen as lubricant additives in rapeseed oil. Ind. Lubr. Tribol. **64**(6), 315–320 (2012)
47. Wu, X.H., Gong, K.L., Zhao, G.Q., Lou, W.J., Wang, X.B., Liu, W.M.: MoS_2/WS_2 quantum dots as high-performance lubricant additive in polyalkylene glycol for steel/steel contact at elevated temperature. Adv. Mater. Interfaces **5**(1), 1700859 (2017)
48. Li, Y., Zhang, S.W., Ding, Q., Tang, J.Z., Qin, B.F., Hu, L.T.: The extreme pressure and lubricating behaviors of potassium borate nanoparticles as additive in PAO. Part. Sci. Technol. **37**(8), 932–942 (2018)